

Synthesis, Characterization, Crystal Structures, and Solution Studies of Ni(II), Cu(II) and Zn(II) Complexes Obtained from Pyridine-2,6-dicarboxylic Acid and 2,9-Dimethyl-1,10-Phenanthroline

H. Aghabozorg^{a,*}, E. Sadr-khanlou^b, A. Shokrollahi^b, M. Ghaedi^b and M. Shamsipur^c

^a*Faculty of Chemistry, Tarbiat Moallem University, Tehran, Iran*

^b*Department of Chemistry, Yasouj University, Yasouj, Iran*

^c*Department of Chemistry, Razi University, Kermanshah, Iran*

(Received 23 November 2007, Accepted 28 December 2007)

The homonuclear water-soluble and air stable compounds (dmpH) (H₅O₂) [M(pydc)₂].0.5H₂O (M = Ni(II) (**1**), Cu(II) (**2**), Zn(II) (**3**); pydcH₂ = pyridine-2,6-dicarboxylic acid, dipicolinic acid, dmp = 2,9-dimethyl-1,10-phenanthroline) have been prepared by self-assembly synthesis in aqueous solution at room temperature, and characterized by IR, ¹H NMR, ¹³C NMR, elemental analysis and X-ray diffraction single crystal analyses for **1**, **2** and **3**. The complexes **1-3** represent the isostructural features. Extensive hydrogen bonding interactions involving all aqua ligands, dipicolinate oxygens and lattice water molecules further stabilize the complex units by linking them to form three dimensional polymeric networks. The stoichiometry and stability of the all three complexes in aqueous solution were investigated by potentiometric pH titration.

Keywords: Nickel(II), Copper(II) and Zinc(II), Pyridine-2,6-dicarboxylic acid, 2,9-Dimethyl-1,10-phenanthroline, Crystal structure, Solution study

INTRODUCTION

Inorganic crystal engineering implies the involvement of metals in extended assemblies. The purpose of involving metals may be purely structural, *e.g.*, providing linkages or controlling network connectivity. When considering the involvement of transition metals in crystal engineering, there are principles in coordination chemistry and organometallic chemistry established during several decades. Specifically, the linking of transition metal-containing molecular building blocks can draw upon these principals both for design and synthesis of the molecular units. The existing knowledge base includes information upon predominant coordination

numbers and coordination geometries for a wide variety of transition metal ions.

The research on the metal carboxylates has always been intriguing in that they play important roles not only in synthetic chemistry with the essence of labile coordination modes of carboxylate group, such as architecture of open and porous framework [1,2], but also in biologic activities [3,4] and physiological effects [5].

The metal carboxylate complexes are vastly studied [6-14] and reviewed [15]. The carboxylate ligand can have different binding modes and each of them may play role in the formation of supramolecular assembly [16-18]. The compounds having multiple carboxylic acid groups are good synthons for supramolecular architectures and coordination polymers [7-10].

*Corresponding author. E-mail: aghabozorg@saba.tmu.ac.ir

To succeed in design of the solid materials with desired physical and chemical properties, the necessary prerequisite is capability to predict crystalline architectures from knowledge of chemical composition. Our aim in this work was to combine this well established molecular inorganic chemistry with well established aspects of supramolecular organic chemistry. Specifically, derivatives of arenes used as building blocks impart rigidity and well defined directionality in the propagation of supramolecular assemblies. In order to gain more information about packing features of molecules containing metal chelate and aryl rings, we have studied crystal structure of nickel(II), copper(II) and zinc(II) complexes derivate of 2,9-dimethyl-1,10-phenanthroline and pyridine-2,6-dicarboxylic acid.

EXPERIMENTAL

Materials and General Methods

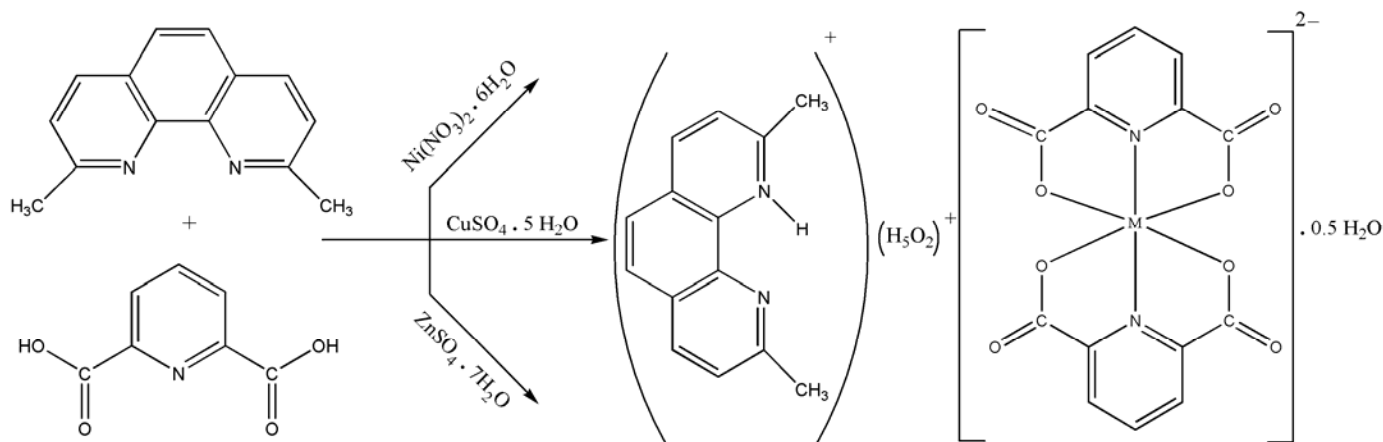
Pyridine-2,6-dicarboxylic acid and neocuproine were purchased from Merck. All other chemicals were obtained from commercial suppliers. Doubly distilled deionized water was used in the procedures when needed. IR spectra were recorded on a Perkin-Elmer 343 and 1720X spectrophotometer using KBr discs. Single-crystal X-ray diffraction experiments were carried out with a Bruker SMART 1000 CCD area detector, using graphite monochromated Mo-K α radiation ($\lambda = 0.71073 \text{ \AA}$, φ - and ω -scans with a 0.5° step in ω , $2\theta < 54$) at 120 K. Low temperature of the crystals was maintained with a

Cryostream (Oxford Cryosystems) open-flow N₂ gas cryostat. Reflection intensities were integrated using SAINT software [19] and semiempirical method SADABS [20]. The structures were solved by direct method and refined by the full-matrix least-squares against F² in anisotropic (for non-hydrogen atoms) approximation. The hydrogen atoms of OH and NH₂ groups as well as water molecules were localized in difference Fourier synthesis, the H(C) atoms were placed in calculated positions. All the hydrogen atoms were refined in riding model with fixed thermal parameters Uiso(H) = 1.2Ueq(Ci), where Ueq(Ci) are the equivalent thermal parameters of the atoms to which corresponding H atoms are bonded. All calculations were performed on an IBM PC/AT using the SHELXTL software [21].

Preparation of (dmpH) (H₅O₂) [M(pydc)₂].0.5H₂O Compounds

The synthetic procedure for the three isostructure complexes is shown in Scheme 1. To the stirring and heating solution of dmp (200 mg 1 mmol) and pydcH₂ (160 mg, 1 mmol) in the mixture of water (10 ml) and methanol (1 ml) was added 1 ml of an aqueous solution of proper salt (0.5 mmol).

All three complexes were characterized by IR spectroscopy. The patterns of IR spectra were exactly the same and show two sets of vibrations due to the aqua and dipicolinate ligands. The $\nu(\text{O-H})$ vibrations belonging to the (H₅O₂)⁺ fragments are observed as broad bands in the 3500-



Scheme 1. Procedure of synthesis of Ni(II), Cu(II) and Zn(II) compounds

3000 cm^{-1} region, typically with two maxima at *ca.*, 3346 and 3082 cm^{-1} . Water in inorganic salts may be classified as lattice water and coordinated water, as the spectra of water molecules are highly sensitive to their surrounding environment, the study of vibrational spectra is a useful tool to distinguish them.

Lattice water normally appears in the 3200-3550 cm^{-1} (antisymmetric and symmetric OH stretching) and 1600-1630 cm^{-1} regions (HOH bendings). The vibration frequencies depict the uncoordinative mode of water fragments. Their broadening to lower energy up to *ca.*, 2300 cm^{-1} is indicative of an extensive H-bonding. Therefore, the $\nu(\text{CH})$ bands overlap with those of $\nu(\text{H}_2\text{O})$ in the spectra of the compound. Several high or medium intensity bands associated with ν_{as} and ν_{s} of the dipicolinate carboxylate groups are also observed in the *ca.*, 1644-1539 and 1426-1283 cm^{-1} spectral ranges, respectively. The most intense bands are rather sharp and usually exhibit absorbance maxima at *ca.*, 1638-1620 (ν_{as}) and 1373 cm^{-1} (ν_{as}). The later one could be also belong to the bending vibrations of methyl groups of $(\text{dmpH})^+$.

There are several similarity between these nickel(II), copper(II) and zinc(II) dipicolinate complexes and other reported ones except the transitions due to the substituent parts [22-28]. This indicates similar metal coordination environments and those inter-atomic interactions are independent on counter cations.

According to the prediction [23-24], the strong peak measured at 1740 cm^{-1} would correspond to Zundel ions. The modes at 1122 and 1740 cm^{-1} appear clearly as a combination of the O-H⁺-O proton stretch and of the H-O-H bends of the external waters. There also must be another vibration, observed as a shoulder to the previous one and spanning 1600-1540 cm^{-1} in the calculation, attributed to the O-H⁺-O bending in H_5O_2^+ and also bending mode in water, this peak should be coupled with C=O vibrational mode. The similarity of IR data supports the idea that these compounds could be isostructure.

The NMR spectroscopy was done for Zn(II) complex. The ¹H and ¹³C NMR spectra show $(\text{pydc})^{2-}$ and $(\text{dmpH})^+$ fragments in the Zn(II) complex in 2:1 molar ratio. Proton resonances have been appeared at 8.43 and 7.73 ppm for $(\text{pydc})^{2-}$ and at 8.11, 8.02 and 2.78 ppm for $(\text{dmpH})^+$, respectively. In the ¹³C NMR spectrum, the resonance at 158.307, 142.852, 134.801, 126.904, 125.902, 125.801 and 21.488 ppm is assigned to $(\text{dmpH})^+$ and the remaining ¹³C

NMR resonances (166.883, 145.677, 140.944 and 125.439 ppm) clearly indicate the presence of (pydcH_2) derivative ligands.

Potentiometric pH Titrations

All potentiometric pH measurements were made on solutions in a 75-ml double-walled glass vessel using a Model 691 Metrohm pH/Ion meter with a combined glass-calomel electrode and Titrionic model T23680. The temperature was controlled at 25.0 ± 0.1 °C by circulating water through the jacket, from a constant-temperature bath (home made thermostat). The cell was equipped with a magnetic stirrer and a tightly fitting cap, through which the electrode system and a 10-ml capacity Metrohm piston burette were inserted and sealed with clamps and O-rings. The atmospheric CO₂ was excluded from the titration cell with a purging steam of purified nitrogen gas. The concentrations of dmp and pydc were 2.87×10^{-3} and 2.50×10^{-3} M, respectively, for the potentiometric pH titrations of pydc and pydc + dmp, in the absence and presence of 1.25×10^{-3} M of M²⁺ ions. A standard carbonate-free KOH solution (0.098 M) was used in all titrations. The ionic strength was adjusted to 0.1 M with KNO₃. Before an experimental point (pH) was measured, sufficient time was allowed for the establishment of equilibrium. The protonation constants of ligands and stability and hydrolysis constants of their metal complexes were evaluated using the program BEST described by Martell and Motekaitis [29]. The value of $K_w = [\text{H}^+][\text{OH}^-]$ used in the calculations was $10^{-13.78}$ [30].

RESULTS AND DISCUSSIONS

We have extended the concept of using ionic hydrogen bonds to create layers of molecules from purely organic compounds to complexes that contain both organic molecules and transition metals. Specifically, we have used transition metals in the 2+ oxidation state (*e.g.*, Cu²⁺) to create coordination compounds that contain two pyridine-2,6-dicarboxylate ion, a compound that behaves as a tridentate ligand by binding metals at the pyridyl nitrogen and at the two carboxylate groups, and a protonated 2,9-dimethyl-1,10-phenanthroline.

The detected crystal system for these isomorphous

compounds is centric orthorhombic in *Fddd* space group, number 70. The Hermann-Mauguin and Schoenflies representative are *mmm* and *D_{2h}*, respectively.

An important feature of these crystal structures are the presentation of (dmpH)⁺ and H₅O₂⁺ counter cations and complexation of doubly deprotonated (pydc)²⁻ as a tridentate ligand. The lattice consists of [M(pydc)₂]²⁻ anionic complexes (M = Ni(II), Cu(II), Zn(II)), 2,9-dimethyl-1,10-phenanthroline cation, H₅O₂⁺ fragment and the water of

crystallization. The presence of cationic part facilitate the proton transfer process and, therefore, the formation of the complex of M(II).

Table 1 lists the details of the crystallographic experiments and computations. Selected inter-atomic distances, bond angles and torsion angles are shown in Table 2. The intermolecular hydrogen bonds are given as Table 3.

The asymmetric unit of compound, (dmpH) (H₅O₂) [Cu(pydc)₂].0.5H₂O, which is isostructural with the

Table 1. Crystal and Structure Refinement Data for Compound **1-3**

	Nickel(II) complex, 1	Copper(II) complex, 2	Zinc(II) complex, 3
Empirical formula	C ₂₈ H ₂₄ N ₄ O ₁₀ Ni	C ₂₈ H ₂₅ N ₄ O _{10.5} Cu	C ₂₈ H ₂₅ N ₄ O _{10.5} Zn
Formula weight	635.22	649.16	650.89
Temperature (<i>T</i> , K)	120(2)	120(2)	120(2)
Wavelength (λ , Å)	0.71073 (Mo K α)	0.71073 (Mo K α)	0.71073 (Mo K α)
Crystal system	Orthorhombic	Orthorhombic	Orthorhombic
Space group	<i>Fddd</i>	<i>Fddd</i>	<i>Fddd</i>
Unit cell dimension (Å, °)	<i>a</i> = 17.930(3) <i>b</i> = 19.082(3) <i>c</i> = 35.223(6)	<i>a</i> = 17.962(2) <i>b</i> = 19.456(2) <i>c</i> = 34.845(5)	<i>a</i> = 17.8968(9) <i>b</i> = 19.4522(11) <i>c</i> = 35.6085(18)
Volume (Å ³)	12051(3)	12178(3)	12396.5(11)
<i>Z</i>	16	16	16
Density (D _{calcd} , g cm ⁻³)	1.400	1.416	1.395
Absorption coefficient (μ , mm ⁻¹)	0.705	0.7080	0.854
<i>F</i> (000)	5248	5344	5360
Crystal size (mm ³)	0.30 × 0.24 × 0.21	0.40 × 0.30 × 0.2	0.30 × 0.25 × 0.20
Theta (θ) range for data collection (°)	2.43 to 27.12	3.87 to 28	2.55 to 29.04
Index ranges	-22 ≤ <i>h</i> ≤ 22, -24 ≤ <i>k</i> ≤ 24, -44 ≤ <i>l</i> ≤ 44	-223 ≤ <i>h</i> ≤ 20, -25 ≤ <i>k</i> ≤ 25, -46 ≤ <i>l</i> ≤ 39	-21 ≤ <i>h</i> ≤ 24, -26 ≤ <i>k</i> ≤ 26, -40 ≤ <i>l</i> ≤ 48
Reflections collected	26597	16841	18544
Independent reflections	3230 [<i>R</i> _(int) = 0.0502]	3562 [<i>R</i> _(int) = 0.0482]	4052 [<i>R</i> _(int) = 0.0488]
Max. and Min. transmission	0.866 and 0.816	0.847 and 0.671	0.847 and 0.671
Refinement method	Full-matrix least-squares on <i>F</i> ²	Full-matrix least-squares on <i>F</i> ²	Full-matrix least-squares on <i>F</i> ²
Final <i>R</i> indices [<i>I</i> > 2σ(<i>I</i>)]	<i>R</i> ₁ = 0.0921, <i>wR</i> ₂ = 0.2378	<i>R</i> ₁ = 0.0798, <i>wR</i> ₂ = 0.1630	<i>R</i> ₁ = 0.0812, <i>wR</i> ₂ = 0.1877
Largest diff. peak and hole (e Å ⁻³)	0.965 and -0.555	0.949 and -0.483	1.009 and -0.519

Table 2. Bond Lengths (Å) and Angles (°) for Compounds **1-3**

Ni1-O1	2.117(11)	Cu1-O1	2.184(3)	Zn1-O1	2.183(3)
Ni1-O1#1	2.117(11)	Cu1-O1#1	2.184(3)	Zn1-O1#1	2.183(3)
Ni1-O3	2.134(10)	Cu1-O3	2.192(3)	Zn1-O3	2.190(3)
Ni1-O3#1	2.134(10)	Cu1-O3#1	2.192(3)	Zn1-O3#1	2.190(3)
Ni1-N1	1.964(16)	Cu1-N1	1.965(16)	Zn1-N1	2.007(4)
Ni1-N2	1.956(13)	Cu1-N2	1.970(13)	Zn1-N2	2.011(5)
O1-Ni1-O1#1	156.0(5)	O1-Cu1-O1#1	154.20(15)	O1-Zn1-O1#1	153.27(16)
O1-Ni-O3	92.5(4)	O1-Cu1-O3	93.28(13)	O1-Zn1-O3	93.23(13)
O1-Ni-O3#1	92.5(4)	O1-Cu1-O3#1	92.52(13)	O1-Zn1-O3#1	92.95(13)
O1#1-Ni1-O3	92.5(4)	O1#1-Cu1-O3	92.52(13)	O1#1-Zn1-O3	92.95(13)
O1#1-Ni1-O3#1	92.5(4)	O1#1-Cu1-O3#1	93.28(13)	O1#1-Zn1-O3#1	93.23(13)
O3-Ni1-O3#1	156.1(5)	O3-Cu1-O3#1	153.80(15)	O3-Zn1-O3#1	153.05(15)
O1-Ni1-N1	78.0(3)	O1-Cu1-N1	77.10(8)	O1-Zn1-N1	76.63(8)
O1-Ni1-N2	102.0(3)	O1-Cu1-N2	101.92(8)	O1-Zn1-N2	103.37(8)
O1#1-Ni1-N1	78.0(3)	O1#1-Cu1-N1	77.10(8)	O1#1-Zn1-N1	76.63(8)
O1#1-Ni1-N2	10.20(3)	O1#1-Cu1-N2	102.90(8)	O1#1-Zn1-N2	103.37(8)
O3-Ni1-N1	101.9(2)	O3-Cu1-N1	103.10(8)	O3-Zn1-N1	103.47(8)
O3-Ni1-N2	78.1(2)	O3-Cu1-N2	76.90(8)	O3-Zn1-N2	76.53(8)
O3#1-Ni1-N1	101.9(2)	O3#1-Cu1-N1	103.10(8)	O3#1-Zn1-N1	103.47(8)
O3#1-Ni1-N2	78.1(2)	O3#1-Cu1-N2	76.90(8)	O3#1-Zn1-N2	76.53(8)
N1-Ni1-N2	180.0	N1-Cu1-N2	180.0	N1-Zn1-N2	180.000(1)
O1-Ni1-O3-C8	100.3(10)	O1-Cu1-O3-C8	-100.9(3)	O1-Zn1-O3-C8	101.4(3)
O1#1-Ni1-O3-C8	-103.2(11)	O3#1-Cu1-O1-C4	101.6(3)	O3#1-Zn1-N1-C1	89.8(3)
#1: [-x+7/4, -y+7/4, z]		#1: [-x+5/4, -y+9/4, z]		#1: [-x+5/4, -y+9/4, z]	

Table 3. Hydrogen Bonding Geometry for Compound **1-3**

D-H...A	D-H (Å)	H...A (Å)	D...A (Å)	<DHA (°)
Nickel(II) compound (1)				
N3-H3B...N4	0.88	2.54	2.848 (12)	101
N3-H3B...O3#1	0.88	2.02	2.775(12)	144
N4-H18A...O3#2	0.95	2.19	3.036(11)	148
O1W-H1WA...O2	0.91	1.68	2.59(2)	174
O1W-H1WC...O1W#3	0.93	1.66	2.60(2)	180
O2W-H2WA...O4	0.86	1.82	2.676(15)	170
O2W-H2WB...O2W#4	0.91	1.66	2.57(2)	180
C2-H2A...O4#5	0.95	2.46	3.29(2)	148
C6-H6A...O2#6	0.95	2.42	3.249(14)	146
C17-H17C...O1W#7	0.95	2.71	3.655(14)	164

Table 3. Continued

#1: $x-1/2, y-1/2, -z$; #2: $-x+3/2, -y+1/2, z+3/2$; #3: $-x+5/4, -y+5/4, z$; #4: $-x+9/4, -y+5/4, z$; #5: $x-1/4, -y+3/2, z+1/4$; #6: $x+1/4, -y+3/2, z-1/4$; #7: $-x+1, -y, -z+2$.				
Copper(II) compound (2)				
N1'-H1'...N2'	1.16	2.14	2.76(2)	110
N1'-H1'...O3#1	1.16	1.98	2.876(12)	130
O1W-H1W1...O4	0.97	1.76	2.701(5)	163
O1W-H2W1...O1W#2	0.97	1.69	2.662(8)	180
O2W-H1W2...O2W#3	0.97	1.733	2.681(15)	165
O2W-H2W2...O2W#4	0.97	1.87	2.736(17)	147
O2W-H3W2...O3W#3	0.97	2.29	2.744(17)	108
O3W-H2W3...N2#5	0.97	2.374	3.232(12)	147
C2-H2A...O4#6	0.95	2.40	3.244(16)	148
C6-H6A...O2#7	0.95	2.37	3.213(6)	147
C6'-H6'A...O3#8	0.96	2.50	3.333(19)	145
#1: $-x+7/4, -y+9/4, z$; #2: $x, -y+9/4, -z+3/4$; #3: $-x+7/4, -y+11/4, z$; #4: $x, -y+11/4, -z+3/4$; #5: $-x+7/4, y, -z+3/4$; #6: $x+1/4, -y+5/2, z-1/4$; #7: $x-1/4, -y+5/2, z+1/4$; #8: $x+3/4, y+1/4, -z+1/2$.				
Zinc(II) compound (3)				
N2S-H2N...N1S	0.97	2.26	2.608(19)	100
N2S-H2N...O3	0.97	2.07	2.856(15)	137
O1W-H1WA...O4#1	0.89	1.91	2.725(4)	152
O1W-H1WB...O1W#2	0.86	1.79	2.649(8)	180
O2W-H2WA...O2#3	0.97	1.68	2.650(7)	174
O2W-H2WB...O2W#4	0.88	1.80	2.657(8)	163
O2W-H2WD...O2W#5	0.96	2.01	2.807(9)	139
O3W-H3WB...N2	0.93	2.41	3.219(10)	145
O3W-H3WB...O1#6	0.93	2.31	2.836(10)	115
O3W-H3WC...O2W	0.94	1.85	2.738(12)	157
C2-H2A...O4#7	0.95	2.45	3.293(6)	147
C6-H6A...O2#8	0.95	2.42	3.258(6)	147
C9-H9SA...O3#8	0.95	2.67	3.568(6)	156
#1: $-x+5/4, y, -z+1/4$; #2: $-x+5/4, -y+9/4, z$; #3: $-x+3/4, y-1/2, -z+1/4$; #4: $-x+5/4, -y+5/4, z$; #5: $x, -y+5/4, -z+1/4$; #6: $-x+7/4, y, -z+3/4$; #7: $x-1/4, -y+2, z-1/4$; #8: $x+1/4, -y+2, z+1/4$.				

corresponding nickel(II) and zinc(II) complexes is presented in Fig. 1. The metal center is hexacoordinated by two nitrogen atoms of two pyridine rings and four carboxylate oxygen atoms of two (pydc)²⁻ tridentate ligands.

The nitrogen atoms occupy the horizontal positions with N1-Cu1-N2 bond angle equal to 180.0°. The metal-nitrogen bond lengths are in the same distance. The remaining

equatorial sites are occupied by the oxygen atoms, which due to the bond angles O1-Cu1-O1A and O3-Cu1-O3A form the flattened tetrahedral geometry.

In the following discussion, the (pydc)²⁻ anionic ligands (C1-C2-C3-C1A-C2A-N1) and (C5-C6-C7-C5A-C6A-N2) are will be referred as **A1** and **A2**, respectively. The adjacent disordered (C1'-C2'-C3'-C4'-C5'-N1') and (C5'-C4'-C6'-C7'-

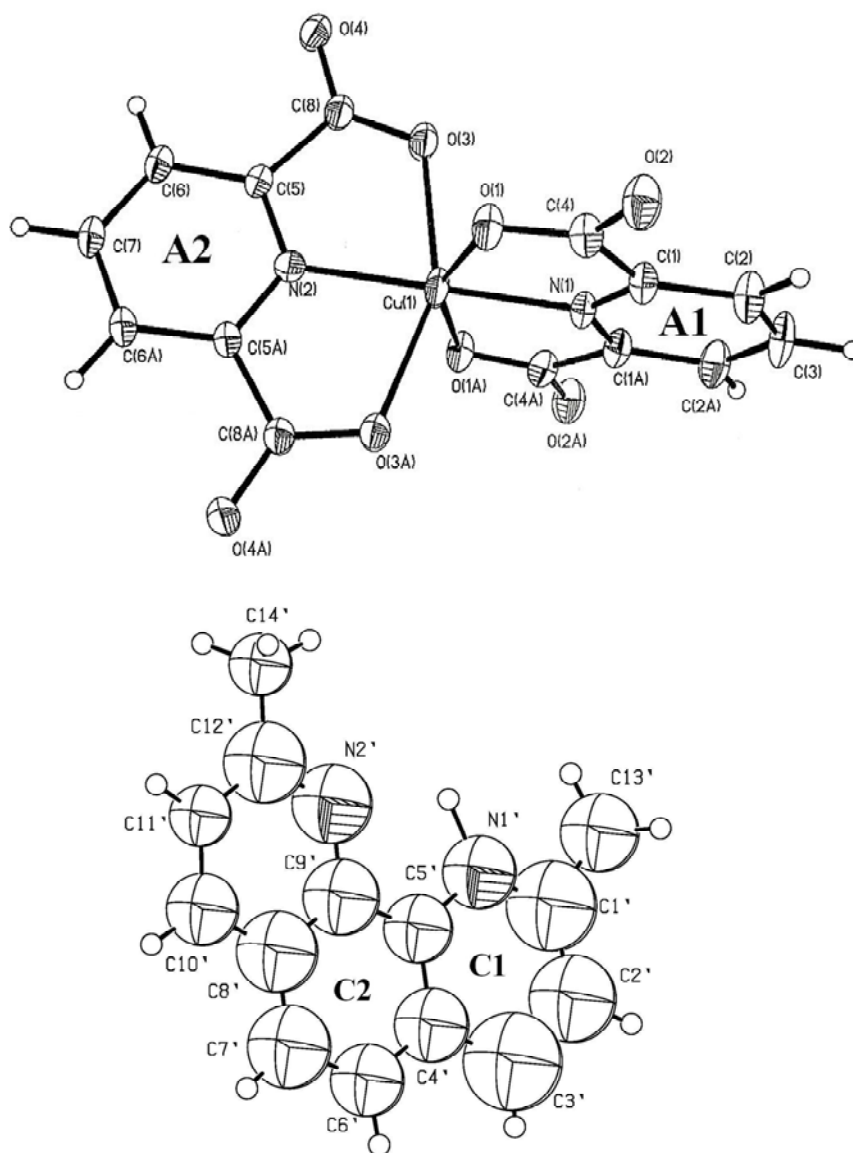


Fig. 1. ORTEP drawing of $[\text{Cu}(\text{pydc})_2]^{2-}$ complex and $(\text{dmpH})^+$. Thermal ellipsoids are drawn at 50% probability.

C8'-C9') rings of $(\text{dmpH})^+$ cation are labeled as **C1** and **C2**.

The metal-nitrogen distances are 1.965(4) and 1.970(5) Å for Cu1-N1 and Cu1-N2, respectively. Comparison between the resulted complex and the previously reported complexes [23,24] indicates the similarity of these Cu-N bonds to the bonds between the Cu(II) center and the nitrogen atom adjacent to the coordinated carboxylate group in $(\text{Hpyda})_2[\text{Cu}(\text{phenc})_2] \cdot 10\text{H}_2\text{O}$ where phenc is phenanthroline-2,9-dicarboxylate.

There are two sets for Cu-O bond lengths, Cu1-O1 and Cu1-O3 which are 2.184(3) Å and 2.192(3) Å, respectively. The remaining two Cu1-O bonds generate by symmetry. The O1-Cu1-O1A and O3-Cu1-O3A bond angles are $154.20(15)^\circ$ and $153.80(15)^\circ$, respectively, providing that the arrangement around the copper center in CuO_4 segment is a distorted tetrahedral (Table 2).

Regarding the O1-Cu1-O3 and O1A-Cu1-O3A angles and O1-Cu1-O3-C8 and O3A-Cu1-O1-C4 torsion angles which are

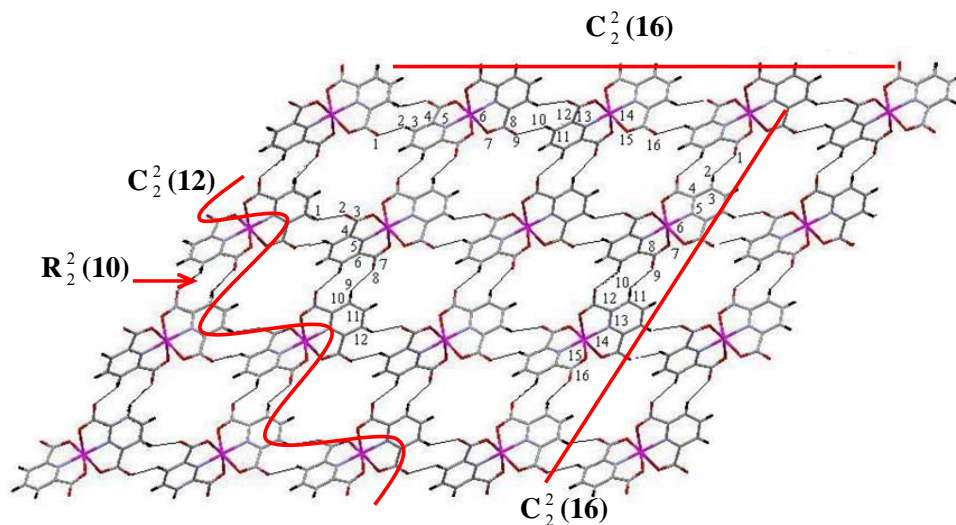


Fig. 2. Graph set descriptors constructing layer, made by C-H...O interactions in $[\text{M}(\text{pydc})_2]^{2-}$.

$93.28(13)^\circ$, $93.28(13)^\circ$, $-100.9(3)^\circ$ and $101.6(3)^\circ$, respectively (Table 2) it is clarified that the two $(\text{pydc})^{2-}$ ligands are almost perpendicular to each other.

In addition to the anionic complex, the highly disordered $(\text{dmpH})^+$ cation also exist in the lattice. By careful analysis of difference maps, the disorder could be resolved into two overlapped symmetry-related fragments. Crystallographic measurements resulted in disordering of all atoms of the $(\text{dmpH})^+$ cation over two positions related by the two-fold axis. They were refined in the isotropic approximation. The resulting overlapped molecules are constrained by symmetry to have equal population parameters of 0.5 for all atoms in the molecule.

The crystal lattice is aggregated through the concert of intermolecular interactions, such as electrostatic attraction between ion pairs, different kinds of hydrogen bonding (O-H...O, N-H...O, C-H...O) and π - π stacking interactions.

The anionic complexes are related to each other forming a wavy chain which is presented in Fig. 2. The operator of such one dimensional aggregate is strongly weak C-H...O interaction. Two C-H...O type interactions are responsible for hydrogen bonding between neighboring anionic $[\text{Cu}(\text{pydc})_2]^{2-}$ complexes. Each of the four free uncoordinated carboxylates oxygen atoms are linked as a bifurcated acceptor to another $[\text{Cu}(\text{pydc})_2]^{2-}$ unit and water fragments *via* hydrogen bonding interactions (Table 3). Considering the D-H...A distances $3.244(16)$ Å for (C2-H2A...O4) and $3.213(6)$ Å for (C6-

H6A...O2), these intermolecular interactions could be investigate as significant ones.

The graph set descriptors belong to these chain forming interactions could be studied in two ways. Each of the C-H...O hydrogen bonds make an infinite chain of the anionic complex, and when come in concert make a ring motif. All graph set descriptors, $R_2^2(10)$, $C_2^2(12)$ and $C_2^2(16)$ are shown in the Fig. 2.

Moreover, each anionic complex is hydrogen bonded to the zundel ions $[(\text{H}_5\text{O}_2)^+]$ by a strong O-H...O interaction and made an endless zigzag like chain (Fig. 3) in which $C_3^3(12)$ graph set descriptors are formed in different directions. It is obvious that the electrostatic attraction between $[\text{Cu}(\text{pydc})_2]^{2-}$ and H_5O_2^+ , could be regarded as an electro motif force in construction of such infinite chains.

The other set of hydrogen bonding patterns included N-H...O and C-H...O, are held between the $(\text{dmpH})^+$ and its counter anion. The hydrogen bond acceptor atom in both interactions is the coordinated O(3), N1'-H1'...O3#1 [#1: $-x+7/4, -y+9/4, z$], C6'-H6'A...O3#8 [#8: $x+3/4, y+1/4, -z+1/2$], so the acceptor bifurcated hydrogen bond occur. The resulting network is very complicated due to the participation of the strong disorder $(\text{dmpH})^+$.

In addition to hydrogen bondings, the crystal packing is influenced by π - π stacking interactions involving the $(\text{dmpH})^+$ ion (Fig. 4). The intercentroid distances shows the wide variety of π - π stacking interactions all over the lattice, making

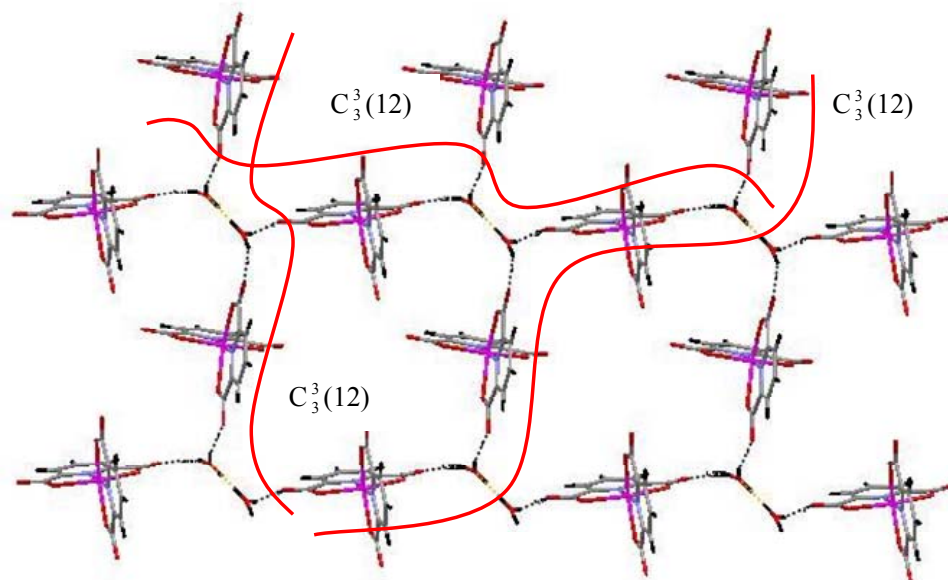


Fig. 3. Graph set descriptors made by O-H...O interactions between zundel ion and $[M(\text{pydc})_2]^{2-}$.

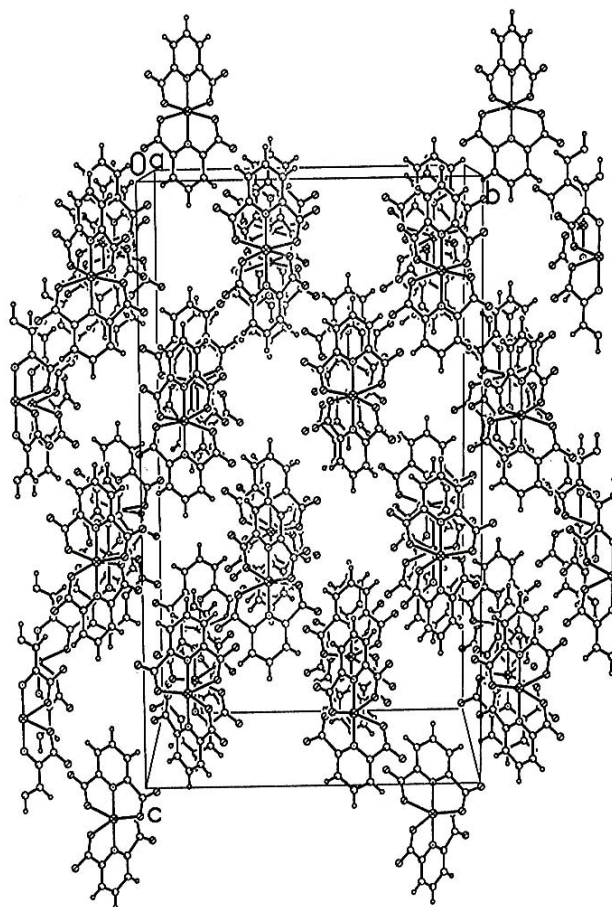


Fig. 4. Packing diagram of $[M(\text{pydc})_2]^{2-}$ complex, cations and water molecules are omitted for clarity.

Table 4. π - π Interactions, Intercentroid and Interplanar Distances Between Mean Plane of Anions and 2,9-Dimethyl-1,10-Phenanthroline Frameworks

π - π Interactions	Intercentroid distance (Å)	Interplanar distance (Å)	Dihedral angle, α (°)	Slipping angle, β (°)	Slipping angle, γ (°)
A1 ... C1 _(a, b)	3.456(10)	3.363(5)	5.41	13.43	10.25
A1 ... C1 _(c, d)	3.377(10)	3.157(5)	5.41	20.78	17.53
A1 ... C2 _(c, d)	3.518(9)	3.211(5)	1.16	23.49	24.13

A: Indicates the mean plane of the pyridine-2,6-dicarboxylate framework in the anion.

A1: N1-C1-C2-C3-C2s-C1s

C: Indicates the mean plane of the 2,9-dimethyl-1,10-phenanthroline framework in the cation.

C1: N1'-C1'-C2'-C3'-C4'-C5'; **C2**: C4'-C5'-C9'-C8'-C7'-C6'

a: $-x+2, -y+5/2, -z+1/2$; **b**: $x-3/4, y-1/4, -z+1/2$; **c**: $x-1/2, y-1/2, z$; **d**: $-x+7/4, -y+0.4, z$.

a three dimensional framework. The variation of values in different sites of the lattice, which could be attributed to the spatial disordering of huge $(\text{dmpH})^+$ ion. The more important aromatic interactions are between **A1-C1** and **A1-C2** (Table 4). The intercentroid distance between **A1-C1** and **A1-C2** are in 3.377-3.518 Å range which increase the possibility of face to face π - π stacking interactions between cation and anionic complex. The least interplanar distances of **A1-C1** and **A1-C2** are 3.157 and 3.211 Å, respectively. Figure 5 represents intercentroid distances. These orientations maximize π - π stacking interactions between **A1**, **C1** and **A1**, **C2** in the crystal lattice.

In addition to the above intermolecular interacting modes, there is an intramolecular interaction between the nitrogen atoms of $(\text{dmpH})^+$ cation.

There are also hydrogen bonding interaction between water molecules ($\text{O2W-H1W2}\cdots\text{O2W}$, $\text{O2W-H2W2}\cdots\text{O2W}$) which result in the cyclic tetramer water clusters. The disordered O3W molecule is attached to O2W *via* ($\text{O2W-H3W2}\cdots\text{O3W}$) hydrogen bonding and makes the hydrogen bonding pattern more complicated. These interactions play an important role in crystal structure as well.

The widespread expansion of all of the intermolecular interactions, mentioned here, through crystal lattice resulted in honey-comb like framework (Fig. 6). Each room is filled by one disordered $(\text{dmpH})^+$, one zundel ion and a tetramer of O2W as is show in Fig. 6b. According to the literature [31],

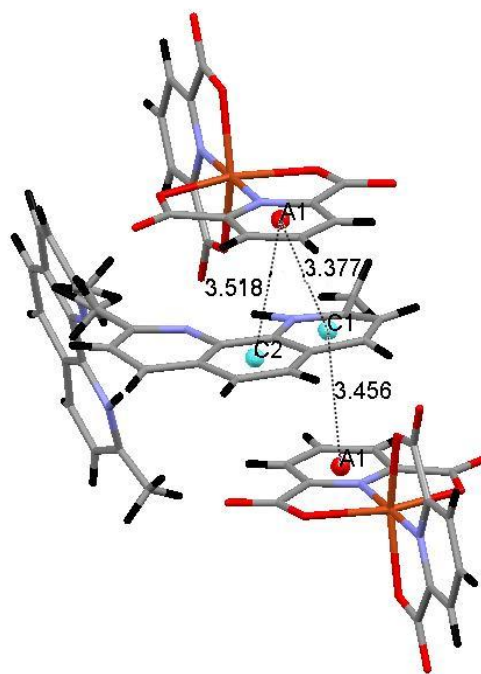


Fig. 5. The intercentroid distances in $(\text{dmpH})(\text{H}_5\text{O}_2)[\text{M}(\text{pydc})_2]\cdot 0.5\text{H}_2\text{O}$.

the best way for the stabilization of $(\text{H}_5\text{O}_2)^+$ cation is the use of crown ethers. In the complexes with crown-ethers, the hydronium cation enters a cavity of crown being linked with oxygen atoms by four hydrogen bonds. Thus, existence of this cation in the cavity of honey-comb could be predictable.

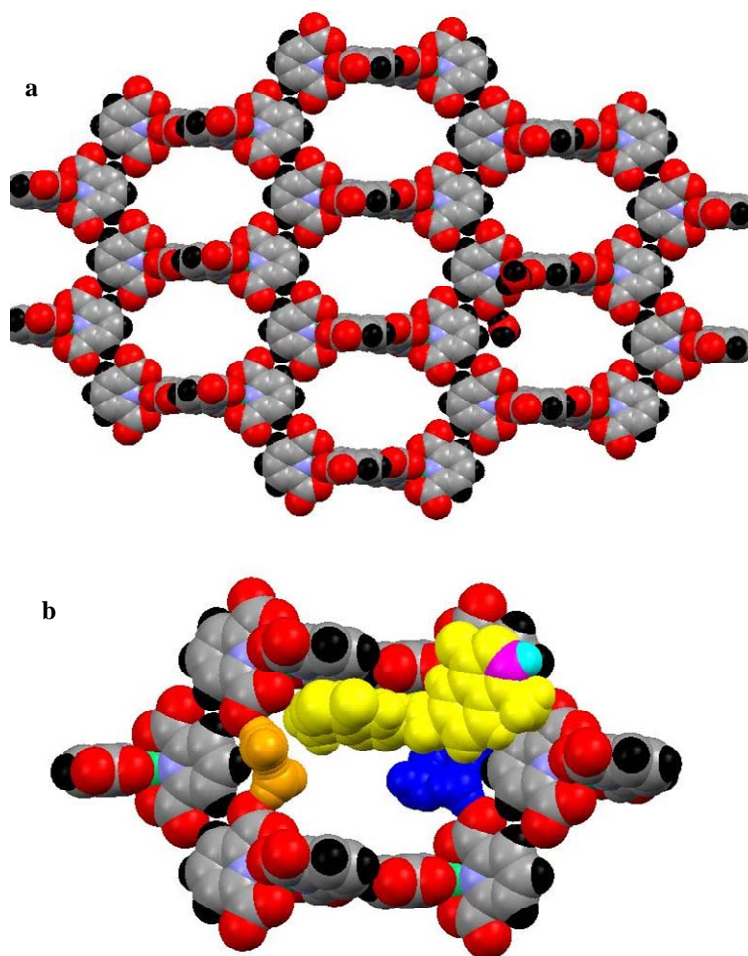


Fig. 6. Honey-comb framework resulted by C-H...O type interactions in the crystal lattice. **a:** the widespread expansion view, **b:** inside of each room. Blue: water tetramer; Orange: $(\text{H}_5\text{O}_2)^+$; Yellow $(\text{dmpH})^+$.

Solution Studies

In preliminary experiments, the fully protonated forms of pydc and dmp, as the building blocks of the self-associated system, were titrated with a standard KOH aqueous solution, to obtain some information about their protonation constants ($K_n^{\text{H}} = [\text{H}_m\text{L}]/[\text{H}_{(m-n)}\text{L}][\text{H}]^n$, the charges are omitted for simplicity), which were calculated by fitting the potentiometric data to the BEST program [29]. We have previously reported the protonation constants of pydc [26]; here, the protonation constants for dmp are given in Table 5. It is noteworthy that the resulting $\log\beta$ values obtained for dmp are in satisfactory agreement with those reported in the literature [32].

The equilibrium constants for the reaction of pydc and

dmp in aqueous solution were evaluated through comparison of the calculated and experimental $p\text{H}$ profiles obtained with both pydc and dmp present, as described before [25,26,33].

The stability constants calculated by fitting of the potentiometric data to the BEST program are listed in Table 6 and the corresponding species distribution diagram is shown in Fig. 7. As is obvious, the most abundant proton-transfer species present at $p\text{H}$ 5.8 and 3.2 are dmpHpydc ($\log K = 3.23$), and dmpHpydcH ($\log K = 2.6$), respectively.

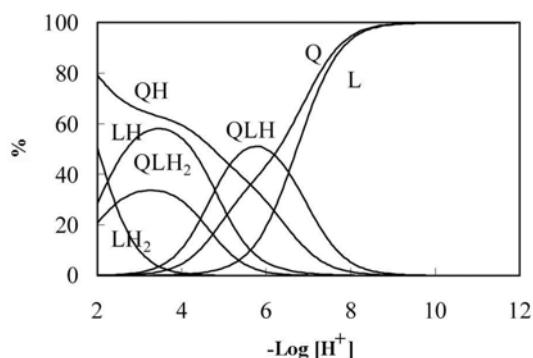
In order to determine the stoichiometry and stability of the Ni(II), Cu(II) and Zn(II) complexes with pydc-dmp association in aqueous solution, the equilibrium potentiometric $p\text{H}$ titration profiles of pydc, dmp and their 1:1 mixture were obtained in the absence and presence of the metal ions. It was

Table 5. Overall Stability Constants of dmp/pydc/M²⁺/H⁺ Binary and Ternary System

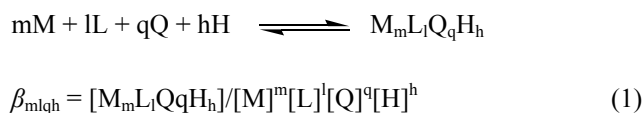
System	m	l	q	h	log β	max%	at pH
dmp	0	0	1	1	6.15	99.9	2.0
Cu-dmp	1	0	1	0	7.12	85.33	2.9
	1	0	2	0	12.10	97.29	>7.2
Ni-dmp	1	0	1	0	3.62	88.09	>10.7
	1	0	1	1	9.75	20.24	2.0
	1	0	2	1	14.03	65.09	6.5
	1	0	2	2	19.56	72.45	2.0
Zn-dmp	1	0	1	0	7.38	50.60	6.7
	1	0	1	1	12.04	45.08	2.0
	1	0	2	0	10.22	33.35	7.3
	1	0	2	1	16.67	41.4	5.5
	1	0	2	2	21.33	54.51	2.0
	1	0	1	-1	-0.37	99.82	>10.9
Cu-pydc	1	1	0	0	7.37	35.6	2.0
	1	1	0	1	8.77	8.8	2.0
	1	1	0	2	10.51	4.7	2.0
	1	2	0	0	13.63	99.8	>5.8
	1	2	0	1	15.74	20.6	2.3
	1	2	0	2	17.63	13.2	2.0
Ni-pydc	1	1	0	0	7.73	42.6	2.2
	1	1	0	1	9.75	42.4	2.0
	1	2	0	0	13.62	97.0	>5.7
	1	2	0	1	15.46	9.0	2.4
Cu-dmp-pydc	1	1	1	0	14.28	negligible	-
	1	2	1	1	30.10	99.59	2.0
	1	1	2	0	22.15	86.8	>11.3
Ni-dmp-pydc	1	2	1	0	14.34	negligible	-
	1	2	1	1	21.21	99.13	2.0
	1	2	1	0	30.79	negligible	-
	1	1	2	0	24.98	99.82	>9.4
Zn-dmp-pydc	1	1	1	0	14.90	negligible	-
	1	1	1	1	15.99	negligible	-
	1	2	1	0	25.62	73.83	4.0
	1	2	1	1	28.00	56.35	2.0
	1	1	2	0	25.42	49.45	7.3
	1	1	1	-1	12.78	97.98	11.9

Table 6. Overall Stability Constants and Stepwise Recognition Constants for Interaction of pydc with dmp at 25 °C and $\mu = 0.1 \text{ M KNO}_3$

Stoichiometry			log β	Equilibrium quotient K	logK	max%	at pH
dmp	pydc	h					
1	1	1	9.38	$[\text{dmpypydcH}]/[\text{dmpH}][\text{pydc}]$	3.23	51.0	5.8
1	1	2	13.82	$[\text{dmpypydcH}_2]/[\text{dmpH}][\text{pydcH}]$	2.60	33.60	3.2

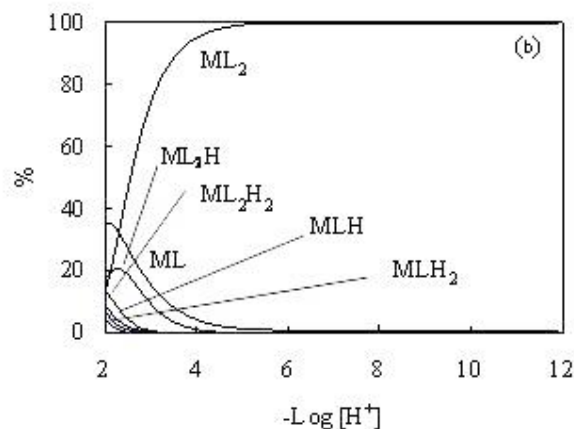
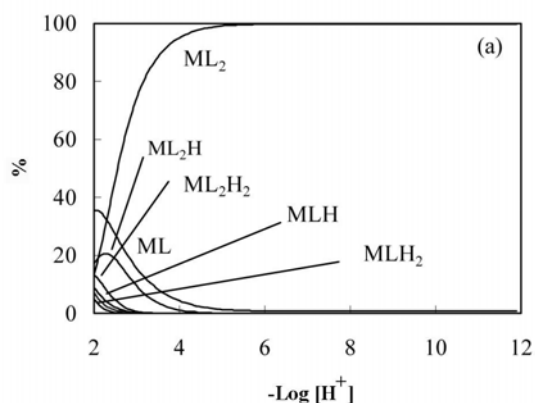

Fig. 7. Distribution diagram of proton transfer interaction between dmp (Q) and pydc (L).

found that, in all cases, the corresponding titration curves depressed significantly in the presence of M^{2+} ion. The cumulative stability constants for the resulting M^{2+} ion complexes, β_{mlqh} , are defined by Eq. (1) (charges are omitted for simplicity),



where M is Ni^{2+} , Cu^{2+} and Zn^{2+} ion, L is pydc, Q is dmp and H is proton, and m, l, q and h are the respective stoichiometric coefficients. Since the ligand and complex activity coefficients are unknown, the β_{mlqh} values are defined in terms of concentrations. The errors are minimized by the use of a high constant ionic strength (0.1 M KNO_3) and low ligand concentration (in the order of 10^{-3} M).

The cumulative stability constants were evaluated by fitting the corresponding pH titration curves to the program BEST and the resulting values for the most likely complexed


Fig. 8. Distribution diagrams of pydc(L)/M binary systems. M = Ni^{2+} (a) and Cu^{2+} (b).

species in aqueous solutions are also included in Table 5. The corresponding values for Zn-pydc have been reported previously [25]. The corresponding species distribution diagrams for dmp and pydc + dmp in the presence of M^{2+} ions are shown in Figs. 8-10.

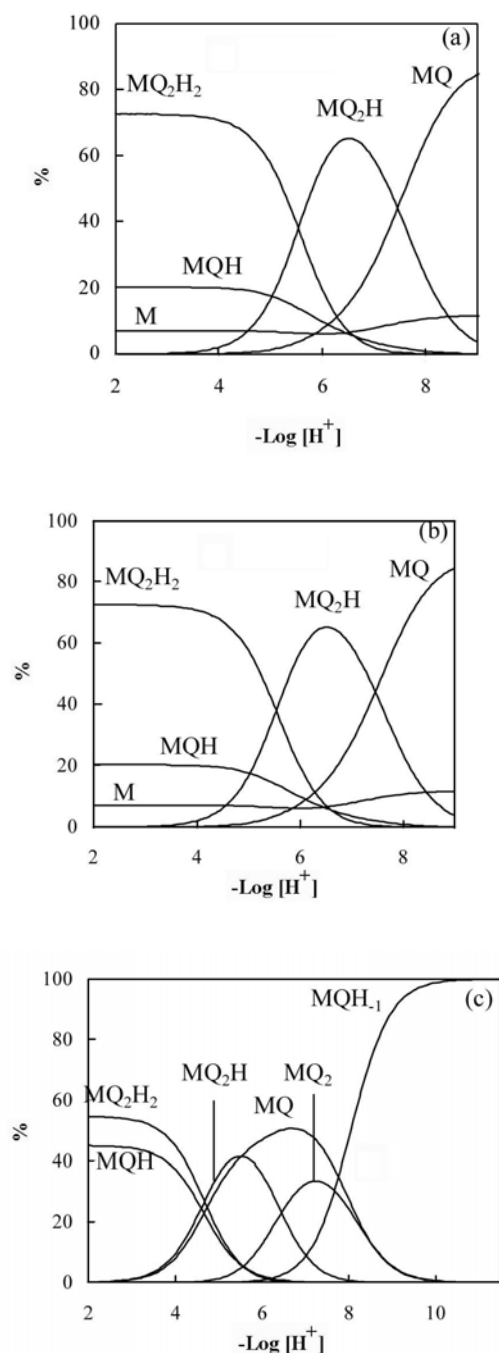


Fig. 9. Distribution diagrams of dmp (Q)/ M binary systems. M = Ni²⁺ (a), Cu²⁺ (b) and Zn²⁺ (c).

As it seen from Table 5 and Figs. 8 and 9, the most likely species in the case of pydc in presence of Ni²⁺ and Cu²⁺ are: NiL, NiLH, NiL₂, NiL₂H, CuL, CuLH, CuLH₂, CuL₂, CuL₂H and CuL₂H₂ and for dmp in presence of Ni²⁺, Cu²⁺ and Zn²⁺

are: NiQ, NiQH, NiQ₂H, NiQ₂H₂, CuQ, CuQ₂, ZnQ, ZnQH, ZnQ₂, ZnQH₁ and ZnQ₂H₂. In the pydc-dmp-M systems, the most likely species are: NiL₂QH, NiLQ₂, CuL₂QH, CuLQ₂, ZnL₂Q, ZnL₂QH, ZnLQ₂ and ZnLQH₁. A comparison between the stoichiometry of the crystalline complex and that of the most abundant species detected in solution clearly revealed that the ML₂QH, as one of the most abundant species existing in aqueous solution, possesses a stoichiometry exactly similar to that of the (dmpH) (H₅O₂) [M(pydc)₂].0.5H₂O complex obtained in solid state.

CONCLUSIONS

We have demonstrated that the pydcH₂ and dmp, providing the proton transfer opportunity, can be used as an appropriate starting material to synthesize a variety of interesting metal-organic compounds, showing interesting intermolecular interacting behavior. Formation of Ni(II), Cu(II) and Zn(II) complexes in solid state are examples of contribution of acidic fragment to the complexation and basic fragment to providing the appropriate intermolecular interactions. Different non-covalent interactions such as ion-pairing, π - π stacking and hydrogen bonding play important roles in the construction of extended networks in the crystal systems as can be observed in Ni(II), Cu(II) and Zn(II) complexes. The formation of these three complexes in solution with stoichiometries very close to those of the solid state is strongly supported by the results of the potentiometric pH titration studies in aqueous solutions.

Supplementary Material

Crystallographic data for the structural analysis have been deposited with the Cambridge Crystallographic Data Centre, CCDC No. 601617, 601616 and 601621 for Ni(II), Cu(II) and Zn(II) complexes, respectively. Copies of this information may be obtained free of charge from the Director, CCDC, 12 Union Road, Cambridge, CBZ 1EZ, UK (Fax: +44-1223-336033; email: deposit@ccdc.cam.ac.uk or www: <http://www.ccdc.cam.ac.uk>).

ACKNOWLEDGEMENTS

Tarbiat Moallem and Yasouj Universities are acknowledged for support of this work.

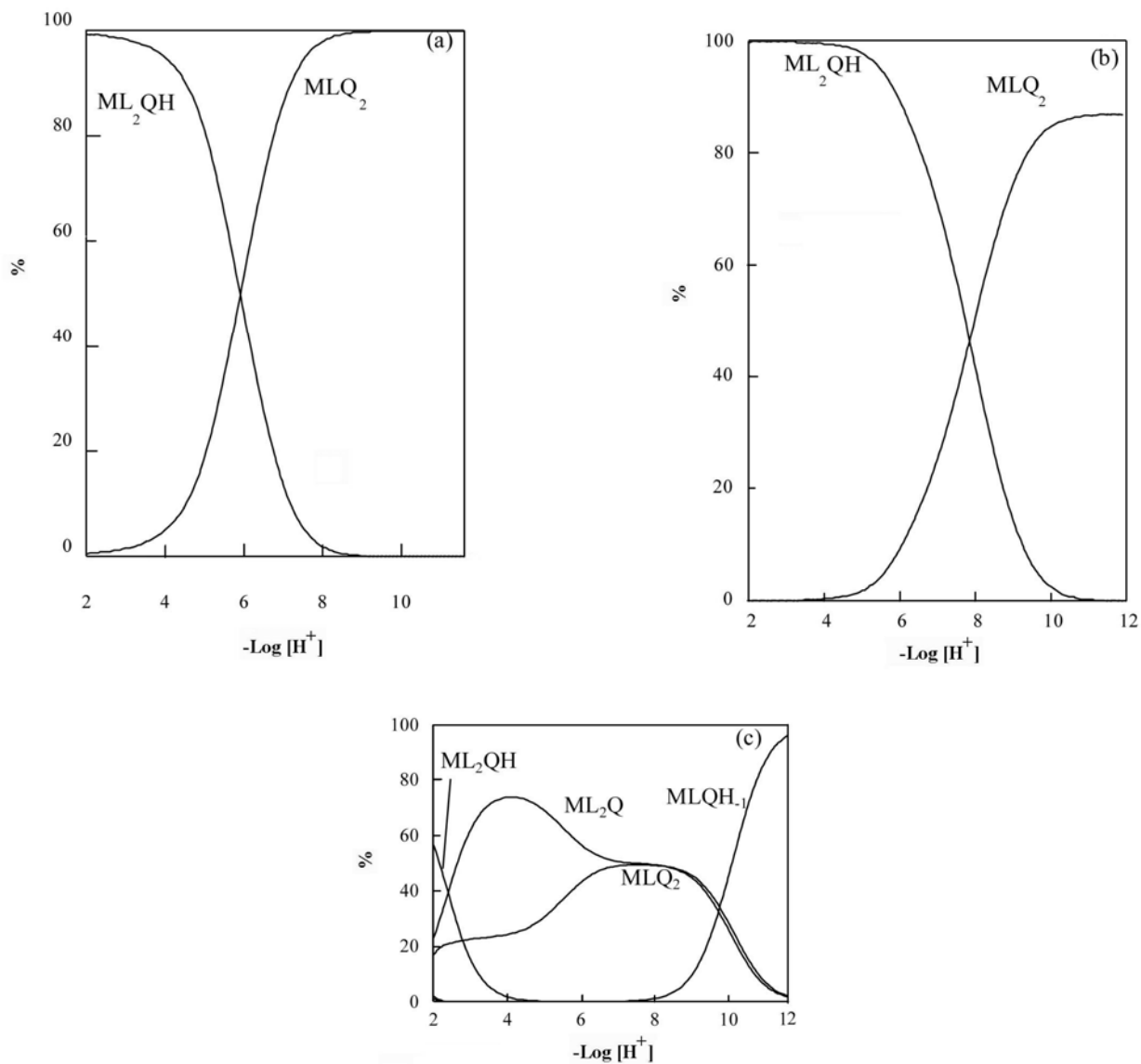


Fig. 10. Distribution diagrams of pydc(L)/dmp(Q)/M ternary systems. $\text{M} = \text{Ni}^{2+}$ (a), Cu^{2+} (b) and Zn^{2+} (c).

REFERENCES

- [1] C.N.R. Rao, S. Natarajan, R. Vaidhyathan, *Angew. Chem. Int. Ed.* 43 (2004) 1466.
- [2] M. Eddaoudi, D.B. Moler, H. Li, B. Chen, T.M. Reineke, M. O’Keeffe, O.M. Yaghi, *Acc. Chem. Res.* 34 (2001) 319.
- [3] Y. Tshuva, S.J. Lippard, *Chem. Rev.* 104 (2004) 987.
- [4] J. Kuzelka, J.R. Farrell, S.J. Lippard, *Inorg. Chem.* 42 (2003) 8652.
- [5] A. Salifoglou, *Coord. Chem. Rev.* 228 (2002) 297.
- [6] H. Aghabozorg, E. Sadr-khanlou, J. Soleimannejad, H. Adams, *Acta Cryst. E63* (2007) m1760.
- [7] H. Aghabozorg, Z. Bahrami, M. Tabatabaie, M. Ghadermazi, J. Attar Gharamaleki, *Acta Cryst. E63* (2007) m2022.
- [8] J. Soleimannejad, H. Aghabozorg, S. Hooshmand, M. Ghadermazi, J. Attar Gharamaleki, *Acta Cryst. E63* (2007) m2389.
- [9] M.A. Sharif, H. Aghabozorg, A. Moghim, *Acta Cryst.*

- E63 (2007) m1599.
- [10] H. Aghabozorg, S. Daneshvar, E. Motyeian, M. Ghadermazi, J. Attar Gharamaleki, *Acta Cryst. E63* (2007) m2468.
- [11] H. Aghabozorg, E. Sadr-khanlou, *Acta Cryst. E63* (2007) m1753.
- [12] H. Aghabozorg, E. Sadr-khanlou, J. Soleimannejad, H. Adams, *Acta Cryst. E63* (2007) m1769.
- [13] H. Aghabozorg, P. Ghasemikhah, M. Ghadermazi, J. Soleimannejad, H. Adams, *Acta Cryst. E63* (2007) m1487.
- [14] H. Aghabozorg, J. Attar Gharamaleki, P. Ghasemikhah, M. Ghadermazi, J. Soleimannejad, *Acta Cryst. E63* (2007) m1710.
- [15] H. Aghabozorg, F. Manteghi, S. Sheshmani, *J. Iran. Chem. Soc.* 5 (2008) 184.
- [16] H. Aghabozorg, F. Mohamad panah, E. Sadr-khanlou, *Anal. Sci.* 23 (2007) x139.
- [17] H. Aghabozorg, F. Ramezanipour, B. Nakhjavan, J. Soleimannejad, J. Attar Gharamaleki, M.A. Sharif, *Cryst. Res. Technol.* 42 (2007) 1137.
- [18] H. Aghabozorg, F. Zabihi, M. Ghadermazi, J. Attar Gharamaleki, S. Sheshmani, *Acta Cryst. E62* (2006) m2091.
- [19] SMART, v. 5.059, Bruker Molecular Analysis Research Tool, Bruker AXS, Madison, Wisconsin, USA.
- [20] G.M. Sheldrick, *SADABS*, Vol. 2.01, 1998, Bruker/Siemens Area Detector Absorption Correction Program, Bruker.
- [21] G.M. Sheldrick, *SHELXTL*, Vol. 5.10, Structure Determination Software Suite, Bruker AXS, Madison, Wisconsin, USA.
- [22] A. Moghimi, M. Ranjbar, H. Aghabozorg, F. Jalali, M. Shamsipur, R.K. Chadah, *J. Chem. Res.* (2002) 1047.
- [23] H. Aghabozorg, F. Zabihi, M. Ghadermazi, J. Attar Gharamaleki, S. Sheshmani, *Acta Cryst. E62* (2006) m2091.
- [24] A. Moghimi, R. Alizadeh, H. Aghabozorg, A. Shokravi, M.C. Aragoni, F. Demartin, F. Isaia, V. Lippolis, A. Harrison, A. Shokrollahi, M. Shamsipur, *J. Mol. Struct.* 750 (2005) 166.
- [25] A. Moghimi, M.A. Sharif, A. Shokrollahi, M. Shamsipur, H. Aghabozorg, *Z. Anorg. Allg. Chem.* 631 (2005) 902.
- [26] A. Moghimi, S. Sheshmani, A. Shokrollahi, M. Shamsipur, G. Kickelbick, H. Aghabozorg, *Z. Anorg. Allg. Chem.* 631 (2005) 160.
- [27] Z. Aghajani, M.A. Sharif, H. Aghabozorg, A. Naderpour, *Acta Cryst. E62* (2006) m830.
- [28] H. Aghabozorg, E. Sadr-Khanlou, *Cryst. Res. Technol.* 43 (2008) 327.
- [29] A.E. Martell, R.J. Motekaitis, *Determination and Use of Stability Constants*, 2nd ed., VCH, New York, 1992.
- [30] G. Schwarzenbach, H. Flaschka, *Complexometric Titrations*, Methuen, London, 1969.
- [31] C. Pettinari, F. Marchetti, R. Pettinari, A. Drozdov, S. Semenov, S.I. Troyanov, V. Zolin, *Inorg. Chem. Commun.* 9 (2006) 634.
- [32] M. Yasuda, K. Sone, K. Yamasaki, *J. Am. Chem. Soc.* 60 (1956) 1667.
- [33] J.B. English, A.E. Martell, R.J. Motekaitis, I. Murase, *Inorg. Chim. Acta* 258 (1997) 183.